Lasers in Surgery and Medicine 29:351–359 (2001)

Analysis of Thermal Relaxation During Laser Irradiation of Tissue

Bernard Choi, MS, PhD,* and Ashley J. Welch, PhD
Biomedical Engineering Laser Laboratory, The University of Texas at Austin, Austin, Texas 78712

Background and Objective: Thermal relaxation time (τ_r) is a commonly-used parameter for estimating the time required for heat to conduct away from a directly-heated tissue region. Previous studies have demonstrated that temperature superposition can occur during multiple-pulse irradiation, even if the interpulse time is considerably longer than τ_r. The objectives of this study were (1) to analyze tissue thermal relaxation following laser-induced heating, and (2) to calculate the time required for a laser-induced temperature rise to decrease to near-baseline values.
Study Design/Materials and Methods: One-dimensional (1-D) analytical and numerical and 2-D numerical models were designed and used for calculations of the time τ_{eff} required for the peak temperature (T_{peak}) to decrease to values slightly over baseline (ΔT_{base}). Temperature values included $T_{peak} = 65$ and 100°C, and $\Delta T_{base} = 5$, 10, and 20°C. To generalize the calculations, a wide range of optical and thermal properties was incorporated into the models. Flattop and gaussian spatial beam profiles were also considered.
Results: 2-D model calculations of τ_{eff} demonstrated that τ_{eff} (2-D) was as much as 40 times longer than τ_r. For a given combination of T_{peak} and ΔT_{base}, a linear relationship was calculated between τ_{eff} (1-D) and τ_r and was independent of optical and thermal properties. A comparison of 1-D and 2-D models demonstrated that 1-D models generally predicted longer values of τ_{eff} than those predicted with a 2-D geometry when the laser spot diameter was equal to or less than the optical penetration depth.
Conclusion: Relatively simple calculations can be performed to estimate τ_{eff} for known values of τ_r, T_{peak} and ΔT_{base}. The parameter τ_{eff} may be a better estimate than τ_r of tissue thermal relaxation during multiple-pulse laser irradiation. Lasers Surg. Med. 29:351–359, 2001.

Key words: effective relaxation time; thermal modeling, finite difference; spatial beam profile; heat conduction

INTRODUCTION

Pulsed laser radiation is used to heat tissue and precisely ablate or coagulate tissue. In laser surgery, the general goal is to selectively heat a desired region of tissue while minimizing collateral thermal damage. The theory of selective photothermolysis proposed by Anderson and Parrish [1] is generally applied to a given situation to determine the appropriate laser pulse duration (τ_p).

From the theoretical analysis of Anderson and Parrish [1], the concept of thermal relaxation time has become a popular term for selection of laser pulse duration. The thermal relaxation time (τ_r) of a heated region of tissue is the time required for the peak temperature rise (ΔT_{peak}) in a heated region of tissue to decrease to 37% of the total rise:

$$\tau_r = \frac{\delta^2}{4\alpha}, \quad (1)$$

where δ is usually the penetration depth (cm). The appropriate value for δ is discussed in more detail in the Discussion section. A common belief is that if τ_p is less than τ_r of the irradiated region, thermal damage is minimized. However, for procedures in which high peak temperatures ($T_{peak} \geq 100$°C) are expected, such as laser skin resurfacing, the temperature value may still be sufficiently large to induce thermal damage after τ_r has elapsed. For example, assuming an initial temperature of 30°C and a laser-induced temperature rise to 100°C, T_{peak} will be approximately (100°C − 30°C)* 0.37 + 30°C = 56°C after τ_r has elapsed. If another laser pulse is applied to the tissue at this point, thermal effects may be more severe due to temperature superposition effects. Complete thermal relaxation of tissue may take several thermal relaxation times [2]. Also, τ_r is applicable only for specific tissue conditions. Tissue optical and thermal properties may change during the laser pulse and for consecutive pulses due to evaporation and tissue denaturation [3,4]; as these properties change, the value of τ_r changes as well.

Several theoretical and experimental studies have shown that temperature superposition can occur even if the time between pulses is several orders of magnitude greater than the thermal relaxation time [5–8]. In

Contract grant sponsor: Air Force Office of Scientific Research through MURI from DDR&E; Contract grant number: F49620-98-1-0480; Contract grant sponsor: Texas Higher Education Coordinating Board; Contract grant number: BER-ATP-253; Contract grant sponsor: Albert and Clemmie Caster Foundation.
*Correspondence to: Bernard Choi, Ph.D., Beckman Laser Institute and Medical Clinic University of California, Irvine 1002 Health Sciences Road East Irvine, CA 92612 Phone: 949-824-3754. E-mail: bchoi@laser.bli.uci.edu
Accepted 30 April 2001

previous measurements of skin radiometric surface temperatures during pulsed CO_2 laser irradiation ($\tau_r \sim 700$ μs) [5], it was demonstrated that elevated temperatures remained for 20–40 ms after the end of a laser pulse. These results indicate that complete tissue thermal relaxation to baseline temperatures is a relatively slow process.

The purpose of this study was to investigate theoretically the thermal response of soft tissue to laser-induced heating. The time required for T_{peak} to decrease to values just above baseline is calculated using a 2-D numerical thermal model. Results of a 1-D analytical solution to the heat conduction equation are compared to those of the numerical model to demonstrate its applicability as a rule-of-thumb estimation for the effective relaxation time (τ_{eff}) of tissue.

MATERIALS AND METHODS

Conduction heat flow is governed by the heat conduction equation. In three dimensions, conduction heat flux q (W/cm^2) is defined as:

$$q = -k\nabla T, \tag{2}$$

where k is thermal conductivity (W/cm/K) and ∇ is the 3-D del operator. In Cartesian coordinates,

$$\nabla = \frac{\partial}{\partial x} + \frac{\partial}{\partial y} + \frac{\partial}{\partial z}$$

The negative sign in Equation (2) is due to the direction of heat conduction; heat always flows from a higher temperature region to a lower temperature region.

In cylindrical coordinates, Equation (2) becomes:

$$\frac{1}{r}\frac{\partial^2 T}{\partial r^2} + \frac{1}{r^2}\frac{\partial^2 T}{\partial \phi^2} + \frac{\partial^2 T}{\partial z^2} + \frac{q_{gen}}{k} = \frac{1}{\alpha}\frac{\partial T}{\partial t}, \tag{3}$$

where q_{gen} is the laser source term (W/cm^3) and α is thermal diffusivity (cm^2/s). If 1-D heat flow is assumed, Equation (2) takes on the following form:

$$\frac{\partial^2 T}{\partial z^2} + \frac{q_{gen}}{k} = \frac{1}{\alpha}\frac{\partial T}{\partial t}.$$

2-D Finite Difference Model

A finite difference solution [9] to the heat conduction equation (Equation (2)) was derived. Cylindrical coordinates were used, resulting in a 2-D axisymmetric tissue geometry (Equation (3)). The tissue was assumed to be homogeneous and its dimensions were 1-cm thickness and 1-cm radial extent. The size of each grid element was 40×20 μm.

Accurate thermal modeling of tissue subjected to relatively high temperatures is difficult due to potential dynamic changes in optical and thermal properties as a function of temperature and water content [3,4]. For the 2-D simulations, we assumed that tissue consisted of 70% water (representative of dermis [10]) and calculated thermal properties from the following equations [11]:

$$\rho = (6.16 \times 10^{-2} W + 0.938)^{-1} \tag{4a}$$

$$c = 2.5 W + 1.7, \tag{4b}$$

$$k = \rho \times 10^{-2}(0.454 W + 0.174), \tag{4c}$$

where ρ is density (g/cm^3), c is specific heat (J/g/K), and W is water content (e.g., for 70% water, $W = 0.7$). For the 1-D simulations (described below), other sets of thermal properties were considered that corresponded to different water contents.

Absorption coefficient (μ_a) values of 10, 100, and 1000 cm^{-1} were selected. These values were representative of those commonly encountered during laser-mediated tissue heating. Intermediate absorption coefficients were used in the 1-D simulations (described below). Three different spot diameters ($\omega_o = 500$ μm, 1.5 mm, and 2.5 mm diameters) were used to take into account various spot size/penetration depth ($\delta = 1/\mu_a$) combinations. Flattop and gaussian spatial beam profiles were considered. For gaussian profiles, ω_o represents the $1/e^2$ diameter.

Pulse durations were chosen to correspond to 1/100th of the thermal relaxation time. This rule for pulse duration selection was chosen since it is reasonable to assume that such a value would generally be considered as sufficient for limiting heat conduction during the pulse.

Radiant exposures were chosen so that the peak temperature T_{peak} at the end of the laser pulse corresponded to either 65 or 100°C. The value of 65°C was chosen because it corresponds to a commonly-cited threshold value for collagen denaturation [7,12,13], although in reality thermal damage is a temperature-time phenomenon [14]. 100°C corresponds to water boiling at atmospheric pressure and is a good estimate of the residual peak temperature in tissue immediately after ablation. The effective relaxation time (τ_{eff}) required for the peak temperature to fall to $\Delta T_{base} = 10$°C above baseline ($T_{baseline} = 22$°C) was calculated for each model run.

1-D Analytical Expression

An advantage of using 2-D models is that they offer more realism than 1-D models. A major disadvantage is the considerably longer computation time required to arrive at a solution. A 1-D equation derived by Anvari et al. [15] from basic principles presented by Carslaw and Jaeger [16] describes 1-D heat flow in a semi-infinite medium with an adiabatic surface boundary condition. This equation was slightly modified to the following form:

$$\Delta T(z,t) = \frac{H_o \mu_a}{2\rho c}\exp(-\xi^2)[\mathrm{erfcx}(\beta - \xi) + \mathrm{erfcx}(\beta + \xi)], \tag{5}$$

where z is depth (cm), t is time (s), H_o is the incident radiant exposure (J/cm^2), $\xi = z/2\sqrt{\alpha t}$, $\beta = \mu_a\sqrt{\alpha t}$, erfc is the complementary error function, and $\mathrm{erfcx}(x) = \exp(x^2)\,\mathrm{erfc}(x)$. Equation (5) is valid for an initial temperature distribution that is proportional to $\exp(-\mu_a z)$; in other words, heat conduction during the pulse is assumed to be negligible. Equation (5) was first compared to results

TABLE 1. Thermal Properties of Various Tissue States

Tissue state	k (W/cm/K)	ρ (g/cm^3)	c (J/g/K)	α(cm^2/s)
100% water	6.28E − 03	1.00E + 00	4.20E + 00	1.50E − 03
70% water	5.01E − 03	1.02E + 00	3.45E + 00	1.42E − 03
0% water	1.86E − 03	1.07E + 00	1.70E + 00	1.02E − 03
Carbon	1.60E − 02	5.00E − 01	6.70E − 01	4.78E − 02

of a 1-D implicit finite difference model in which heat conduction during the pulse was assumed to determine the relative accuracy of this equation. Results of this equation were then compared to those obtained from the 2-D model to determine its suitability for predicting τ_{eff}.

Since the time required to implement Equation (5) was considerably shorter than that required with the 2-D finite difference equations, this equation was applied to a wider variety of cases. Tissue thermal properties were evaluated for four different tissue scenarios: (1) 100% water, (2) 70% water, (3) 0% water, and (4) pure carbon. These sets of thermal properties represented asymptotic limits of tissue states encountered during high-power laser irradiation of tissue and are compiled in Table 1. Equations (4a)–(4c) were used to calculate thermal properties for the first three cases; pure carbon thermal properties were taken from various sources [9,17,18].

The following absorption coefficients were used: 10, 20, 30, 40, 50, 100, 200, 300, 400, 500, 600, 700, 800, 900, and 1000 cm^{-1}. Radiant exposures were chosen so that peak temperatures of 65 and 100°C were obtained by using the following equation:

$$H_o = \frac{\Delta T_{peak} \rho c}{\mu_a}, \tag{6}$$

where $\Delta T_{peak} = T_{peak} - T_{baseline}$ is the peak temperature rise (°C). Equation (6) is simply a 1-D solution to the heat conduction equation at the surface and in the absence of conduction.

The time required for the peak temperature to decrease to ΔT_{base} values of either 5, 10, or 20°C above baseline were calculated. The calculations for 10°C above baseline were directly comparable to the 2-D model runs.

RESULTS

2-D Finite-Difference Model

A total of 36 simulations were run. Figure 1 depicts surface temperature profiles for a representative model run. In the 2-D simulations, $\alpha = 1.42 \times 10^{-3}$ cm^2/s. H_o was

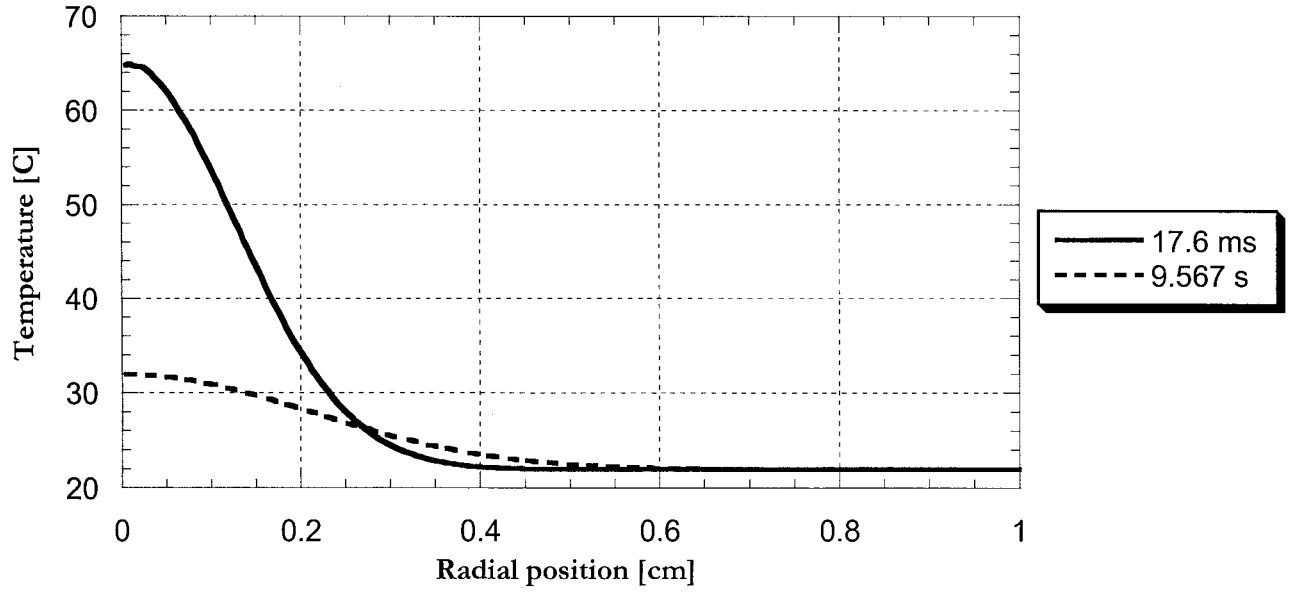

Fig. 1. Surface temperature profiles for a model run at $t = 17.6$ ms (solid line), which is the end of the incident laser pulse, and $t = 9.567$ seconds (dashed line), which is the point in time at which the peak temperature is 32°C. $H_o = 8.16$ J/cm^2, gaussian beam profile, spot radius = 2.5 mm, $\mu_a = 10$ cm^{-1}.

chosen so ΔT_{peak} at the end of a 17.6-ms pulse was 65°C. The time required for T_{peak} to decrease to 32°C was 9.57 seconds. For the experimental conditions simulated in this case, τ_r was 1.76 seconds. Thus, in this example, τ_{eff} was 5.44 times longer than τ_r.

A summary of model results is provided in Table 2. The dimensionless variables Γ and τ represent the ratios ω_o/δ and τ_{eff}/τ_r, respectively. Note that for all but one model run, τ is greater than unity, indicating that the times required for T_{peak} to decrease to 32°C were longer than τ_r.

Figure 2 shows a plot of τ_{eff} calculated for gaussian beam profiles as a function of τ_{eff} for flattop beam profiles. Each coordinate pair represents identical simulated experimental conditions except for the spatial beam profile (Table 2). The solid line represents the boundary at which $\tau_{eff,gaussian} = \tau_{eff,flattop}$. All data points fall below this line, indicating that for a given set of experimental conditions, the value of τ_{eff} required for gaussian temperature distributions to thermally relax is shorter than that for uniform distributions. The discrepancy is larger for longer values of τ_{eff}.

1-D Analytical Equation

Equation (5) was applied to a total of 456 different experimental scenarios. Calculations of τ_{eff} for relatively short pulses ($\tau_p = 0.01\ \tau_r$) were compared to those obtained from 1-D implicit finite difference calculations and agreed to within 1%. Results of all model runs are shown in Figure 3. Note that all calculations of τ_{eff} fall above the solid line, indicating that the times required for T_{peak}

TABLE 2. Summary of 2-D Finite-Difference Model Runs. For These Runs, the Thermal Diffusivity is $\alpha = 1.42 \times 10^{-3}$ cm^2/seconds. μ_a = Absorption Coefficient, ω_o = Beam Diameter, $\Gamma = \omega_o/\delta$, δ = Penetration depth (cm), T_{peak} = Peak Temperature, τ_r = Thermal Relaxation Time, τ_{eff} = Effective Relaxation Time, $\tau = \tau_{eff}/\tau_r$

Model run	Beam type	μ_a (cm^{-1})	ω_o (cm)	Γ (−)	T_{peak} (°C)	τ_r (seconds)	τ_{eff} (seconds)	τ (−)
1	Flattop	10	0.1	1	65	1.76E+00	2.50E+00	1.42E+00
2	Flattop	10	0.1	1	100	1.76E+00	5.59E+00	3.18E+00
3	Flattop	10	0.3	3	65	1.76E+00	9.28E+00	5.29E+00
4	Flattop	10	0.3	3	100	1.76E+00	1.95E+01	1.11E+00
5	Flattop	10	0.5	5	65	1.76E+00	1.51E+01	8.63E+00
6	Flattop	10	0.5	5	100	1.76E+00	3.23E+01	1.84E+01
7	Gaussian	10	0.1	1	65	1.76E+00	1.42E+00	8.11E−01
8	Gaussian	10	0.1	1	100	1.76E+00	3.39E+00	1.93E+00
9	Gaussian	10	0.3	3	65	1.76E+00	5.65E+00	3.22E+00
10	Gaussian	10	0.3	3	100	1.76E+00	1.25E+01	7.09E+00
11	Gaussian	10	0.5	5	65	1.76E+00	9.57E+00	5.45E+00
12	Gaussian	10	0.5	5	100	1.76E+00	2.11E+00	1.20E+01
13	Flattop	100	0.1	10	65	1.76E−02	2.24E+01	1.28E+01
14	Flattop	100	0.1	10	100	1.76E−02	5.62E−01	3.20E+01
15	Flattop	100	0.3	30	65	1.76E−02	2.58E−01	1.47E+01
16	Flattop	100	0.3	30	100	1.76E−02	9.70E−01	5.52E+01
17	Flattop	100	0.5	50	65	1.76E−02	2.59E−01	1.47E+01
18	Flattop	100	0.5	50	100	1.76E−02	9.79E−01	5.58E+01
19	Gaussian	100	0.1	10	65	1.76E−02	1.65E−01	9.40E+00
20	Gaussian	100	0.1	10	100	1.76E−02	3.90E−01	2.22E+01
21	Gaussian	100	0.3	30	65	1.76E−02	3.01E−01	1.71E+01
22	Gaussian	100	0.3	30	100	1.76E−02	8.11E−01	4.62E+01
23	Gaussian	100	0.5	50	65	1.76E−02	3.34E−01	1.90E+01
24	Gaussian	100	0.5	50	100	1.76E−02	1.07E+00	6.12E+01
25	Flattop	1000	0.1	100	65	1.76E−04	7.02E−03	4.00E+01
26	Flattop	1000	0.1	100	100	1.76E−04	2.32E−02	1.32E+02
27	Flattop	1000	0.3	300	65	1.76E−04	7.02E−03	4.00E+01
28	Flattop	1000	0.3	300	100	1.76E−04	2.32E−02	1.32E+02
29	Flattop	1000	0.5	500	65	1.76E−04	6.99E−03	3.98E+01
30	Flattop	1000	0.5	500	100	1.76E−04	2.31E−02	1.32E+02
31	Gaussian	1000	0.1	100	65	1.76E−04	6.75E−03	3.84E+01
32	Gaussian	1000	0.1	100	100	1.76E−04	2.07E−02	1.18E+02
33	Gaussian	1000	0.3	300	65	1.76E−04	7.00E−03	3.99E+01
34	Gaussian	1000	0.3	300	100	1.76E−04	2.30E−02	1.31E+02
35	Gaussian	1000	0.5	500	65	1.76E−04	7.00E−03	3.99E+01
36	Gaussian	1000	0.5	500	100	1.76E−04	2.30E−02	1.31E+02

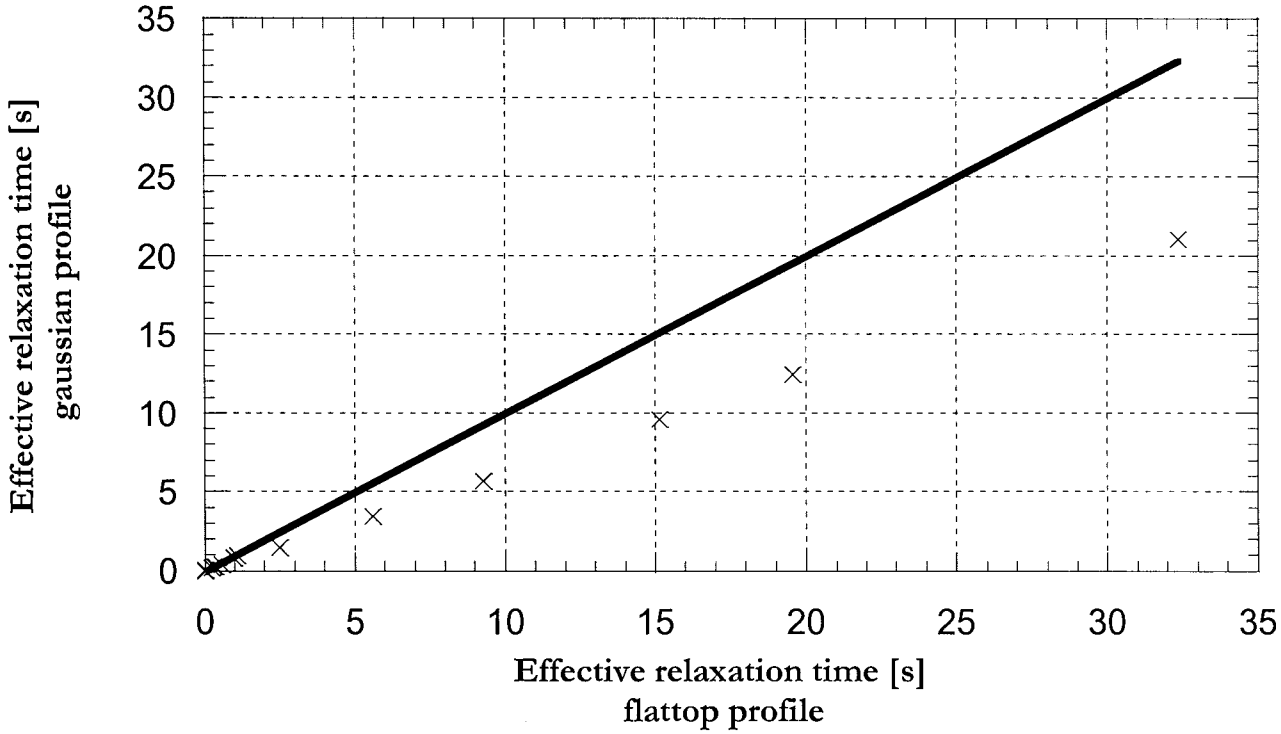

Fig. 2. Log-log plot of effective thermal relaxation time for a gaussian beam profile vs. effective relaxation time τ_{eff} for a flattop beam profile. All points fall below the solid line, indicating that τ_{eff} for a gaussian beam is less than that for a flattop beam. For this plot, τ_{eff} is time required for peak temperature to decrease to 10°C above baseline.

decreasing to values 5–20°C above baseline are longer than τ_r.

In Figure 3, it is evident that for given combinations of peak temperature rise ($T_{peak} = 43$ or 78°C) and final peak temperature above baseline ($\Delta T_{base} = 5$, 10 or 20°C), a plot of τ_{eff} vs. τ_r yields data that fall along straight lines. Average slopes of linear fits are listed in Table 3. The slope of each line dictates the offset of each line on the plot; a larger slope indicates a higher offset. Note that for a given combination of ΔT_{peak} and ΔT_{base}, the linear slopes are identical regardless of the combination of tissue optical and thermal properties used in the model.

Comparison of 2-D and 1-D Model Results

Figure 4 shows τ_{eff} (1-D model)/τ_{eff} (2-D model) as a function of τ_{eff} (2-D model). In general, the 1-D model overpredicts τ_{eff} (e.g., y-axis values greater than unity). This overprediction is associated with the ratio (Γ) of spot size (ω_o) to penetration depth (δ). When $\omega_o \gg \delta$ (e.g., for large Γ), the 1-D solution is accurate at the center of the laser spot, and thus the values of τ_{eff} calculated with the 1-D and 2-D models are comparable (Fig. 5).

DISCUSSION

The main advantage of τ_r is that it is a simple quantity to calculate. It can also be used to adequately predict thermal effects from single-pulse irradiation procedures, such as Port Wine Stain treatment [19]. For cases in which multiple pulses are delivered, such as laser skin resurfacing or laser-assisted blepharoplasties, our results demonstrate that τ_r is not a good indicator for estimating thermal effects (Fig. 3 and Table 2). Model calculations predict that τ_{eff} (2-D) can be as much as 40 times longer than τ_r for peak temperature relaxation from 100 to 32°C for a 22°C baseline temperature; other researchers have estimated comparable values of τ_{eff} [7,8].

Since τ_{eff} can be on the order of 30 seconds (e.g., model run #6 in Table 2), it is necessary to consider the effects of blood perfusion on τ_{eff}. Welch et al. [20] estimated that perfusion has a significant effect on temperatures in normal skin after approximately 100 seconds of laser heating. Thus, the values of τ_{eff} calculated in this study are not expected to differ significantly if blood flow were considered.

van Gemert and Welch [21] demonstrated that the value of δ in Equation (1) depends on $\Gamma = \omega_o/\delta$. For large values of Γ, δ is the penetration depth of light. For small values of Γ, δ is better represented by ω_o. Many laser-based therapeutic procedures involve conditions in which Γ is large, and so δ is the penetration depth. To minimize confusion, in this study we assumed that δ is the penetration depth for all values of Γ.

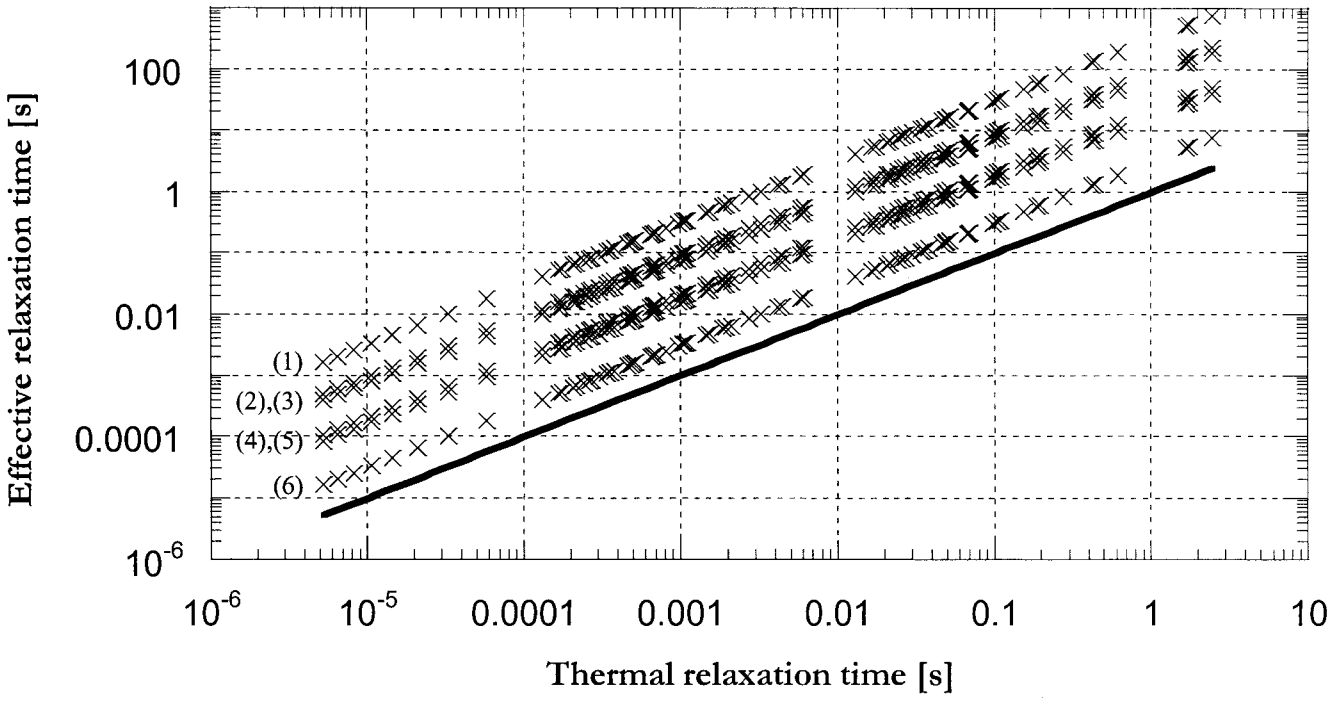

Fig. 3. Log-log plot of effective thermal relaxation time plotted vs. thermal relaxation time for the 456 1-D analytical model runs. All points fall above the solid line, indicating that $\tau_{eff} > \tau_r$. For a given combination of T_{peak} and ΔT_{base}, data points are described by a linear fit. From top to bottom, the temperature values used in the models were (1) $T_{peak} = 100°C$, $\Delta T_{base} = 5°C$; (2) $T_{peak} = 65°C$, $\Delta T_{base} = 5°C$; (3) $T_{peak} = 100°C$, $\Delta T_{base} = 10°C$; (4) $T_{peak} = 65°C$, $\Delta T_{base} = 10°C$; (5) $T_{peak} = 100°C$, $\Delta T_{base} = 20°C$; and (6) $T_{peak} = 65°C$, $\Delta T_{base} = 20°C$.

Data in Figure 2 suggest that for a given parameter set, thermal relaxation is a faster process for incident gaussian beams than for flattop beams. This can be explained by a discussion on radial temperature gradients. Normalized, representative temperature profiles at the end of laser irradiation are shown in Figure 6 for incident gaussian and flattop beams that are 2.5 mm in radius. Initially, at $r = 0$, no net radial heat conduction will occur for the flattop case because the temperatures at adjacent radial positions are equal in magnitude. On the other hand, for the gaussian example, net heat flow away from the central axis occurs almost immediately because adjacent regions (e.g., $r > 0$) are at lower temperatures. The discrepancy between τ_{eff} for gaussian and flattop beams increases as Γ gets larger because, for a given μ_a, as spot size increases, the region of $T = T_{peak}$ during flattop-beam irradiation increases as well. For a gaussian beam, T_{peak} occurs only at the central axis and its location is insensitive to changes in spot size.

TABLE 3. Slope of Linear Fits to Data. ΔT_{peak} = Peak Temperature Rise Above Baseline. ΔT_{base} = Final Temperature Rise Above Baseline

ΔT_{peak} [°C]	ΔT_{base} [°C]	Slope ± SD (−)
43	5	91.2 ± 0.7
43	10	20.2 ± 0.1
43	20	3.1 ± 0.0
78	5	309.3 ± 2.4
78	10	74.2 ± 0.5
78	20	16.0 ± 0.1

Schomacker et al. (7) observed that heat required for ablation during CO_2 laser ablation of in vitro guinea pig skin increased from 4.8 to 6.6 kJ/g as ω_o decreased from 680 to 250 μm. Our model results (Table 2) show that for a given μ_a, τ_{eff} (2-D) decreases as ω_o gets smaller, suggesting that heat loss from the irradiated region is faster for smaller beam diameters. This hypothesis offers a reasonable explanation for why a decrease in ω_o leads to an increase in heat required for ablation.

A plot of τ_{eff} (1-D) calculated using Equation (5) as a function of τ_r (Fig. 3) shows that a 1-D thermal model

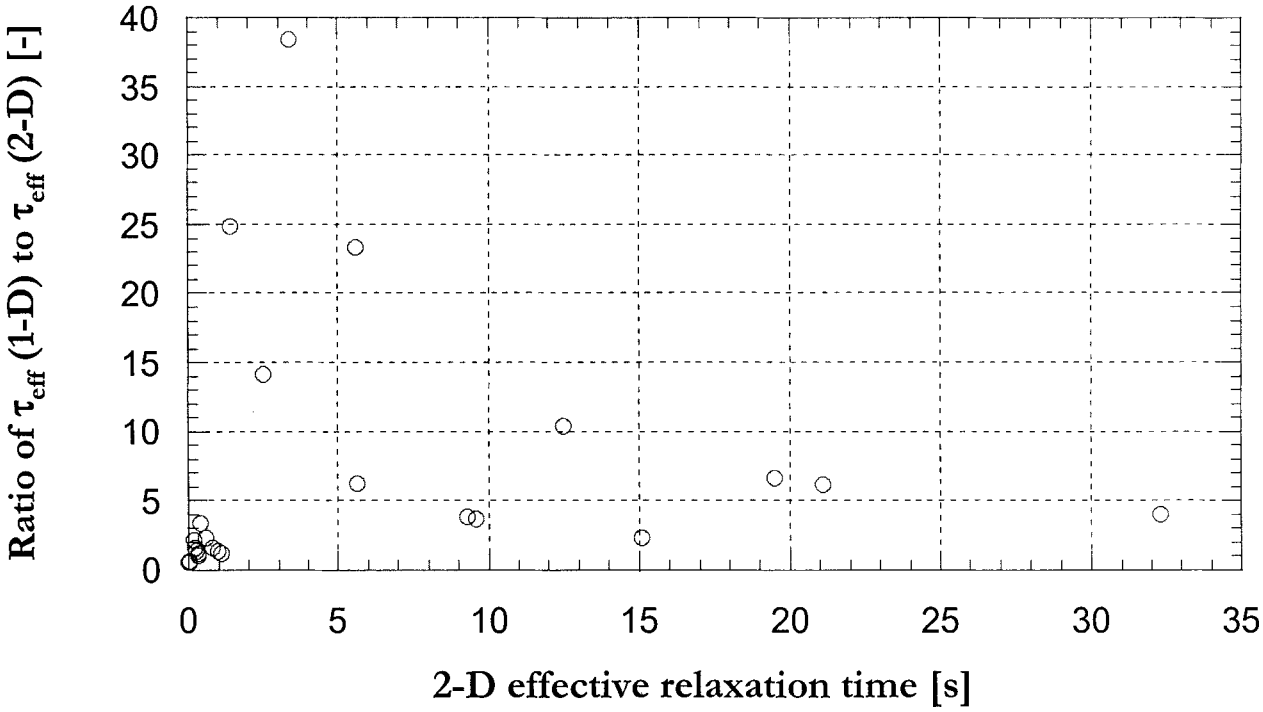

Fig. 4. Ratio of τ_{eff} calculated from 1-D and 2-D models as a function of τ_{eff} calculated from 2-D models.

predicts τ_{eff} (1-D) $> \tau_r$ for the range of τ_r considered in this study. The linear relationship between τ_{eff} (1-D) and τ_r suggests that a simple multiplicative factor can be used to calculate τ_{eff} (1-D). The value of this factor depends solely on ΔT_{peak} and ΔT_{base} and was calculated for six combinations of ΔT_{peak} and ΔT_{base} (Table 3). Further derivation of Equation (5) demonstrates the reason for this linear relationship. For all times $t > 0$, the peak temperature induced by laser light absorption occurs at the tissue surface because the following conditions were assumed during model runs: (1) light scattering was negligible and 2) convective cooling was not considered. Thus, at $z = 0$ and at $t = \tau_{eff}$, Equation (5) becomes

$$\Delta T\ (0, \tau_{eff}) = \frac{H_o \mu_a}{\rho c} \mathrm{erfc}\, x(\beta). \qquad (7)$$

In terms of the models, $\Delta T(0,\tau_{eff})$ is equivalent to ΔT_{base} and the quantity $H_o\mu_a/\rho c$ equivalent to ΔT_{peak}. The term erfcx(β) takes into consideration the dynamic change in peak temperature over time. Thus, Equation (7) takes on the following form

$$\Delta T_{base} = \Delta T_{peak} \mathrm{erfc}\, x(\beta). \qquad (8)$$

Using Equation (1) and $t = \tau_{eff}$, β can be rewritten as

$$\beta = (t = \tau_{eff}) = \mu_a (\alpha\, \tau_{eff})^{1/2} = \frac{1}{2}\left(\frac{\tau_{eff}}{\tau_r}\right)^{1/2}. \qquad (9)$$

Thus, β represents the ratio $\tau = \tau_{eff}/\tau_r$. Since erfcx (β) is a monotonically-decreasing function as β increases, for a given set of values for ΔT_{base} and ΔT_{peak}, there exists a single value for β that satisfies Equation (8). In this situation, β is a constant, so the ratio τ_{eff}/τ_r is also constant. This relationship is true for any combination of optical and thermal properties. Table 3 provides examples of the linear relationship existing between τ_{eff} and τ_r for six combinations of ΔT_{base} and ΔT_{peak}.

A comparison between τ_{eff} values calculated from the 1-D and 2-D models (Fig. 4) indicates that the 1-D model is comparable to or overestimates τ_{eff} (2-D). The amount of overestimation depends on Γ (Fig. 5). As described above, for larger spot sizes, radial heat conduction is not as significant as for smaller spot sizes. For $\Gamma > 10$, τ_{eff} is equivalent for 1-D and 2-D model calculations; this condition is generally satisfied for incisional or ablation procedures. These results show that the 1-D model can at least provide a conservative estimate of the time required between pulses to minimize potentially deleterious effects of temperature superposition. A worst-case value for τ_{eff} can be calculated using a wide range of thermal properties (Equations 4 (a–c), Table 1). Equation (5) is more complex than the equation for τ_r (Equation (1)), but it can still be solved relatively easily using conventional spreadsheet programs.

Since τ_{eff} is linearly related to τ_r, the accuracy of both values suffers from the same limitation in that accurate knowledge of local optical and thermal properties is

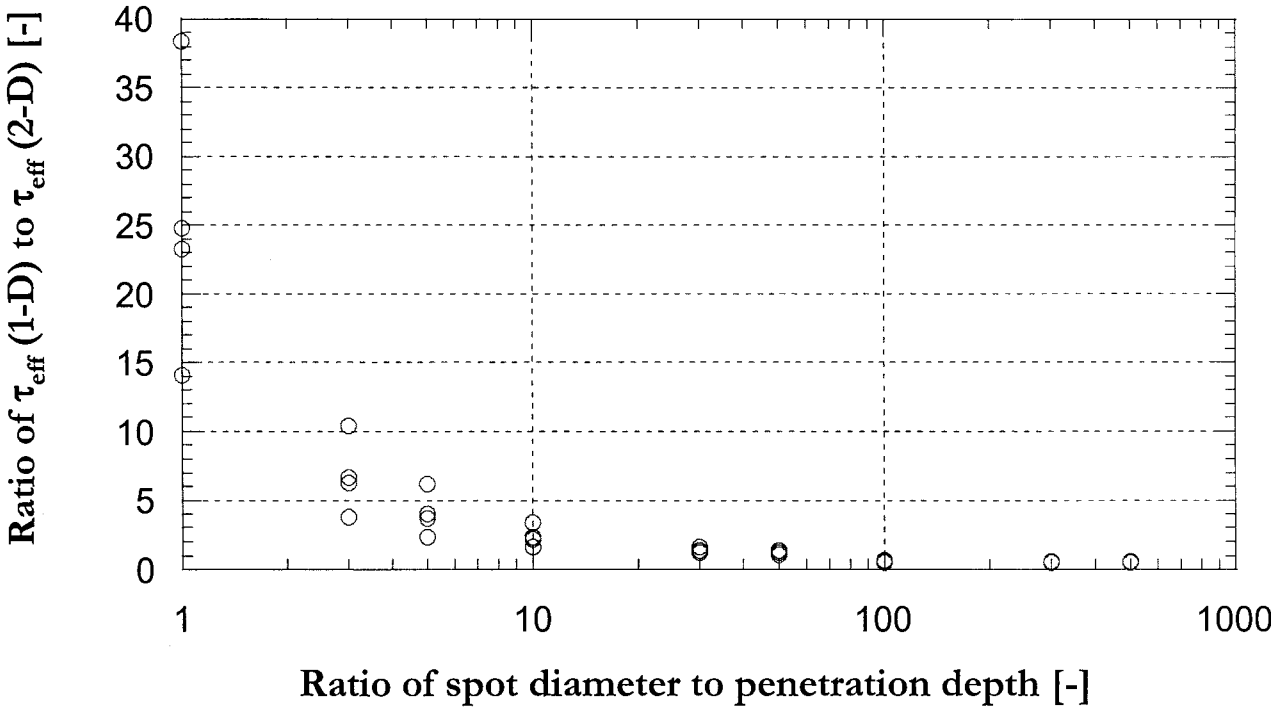

Fig. 5. Semilog plot of ratio of spot diameter and penetration depth vs. τ_{eff} (2-D).

required. In particular, to calculate β, values of μ_a and α must be known. Since τ_{eff} is longer than τ_r, the relative error associated with the uncertainty in a given set of optical and thermal properties is smaller for calculation of τ_{eff} than for τ_r. It is necessary to keep in mind that both τ_{eff} and τ_r are guidelines. The primary purpose of τ_{eff} is to provide an estimate of the time required for heated tissue to cool from T_{peak} to a value ΔT_{base} above baseline, whereas τ_r represents the time required to cool from T_{peak} to a $1/e$ value.

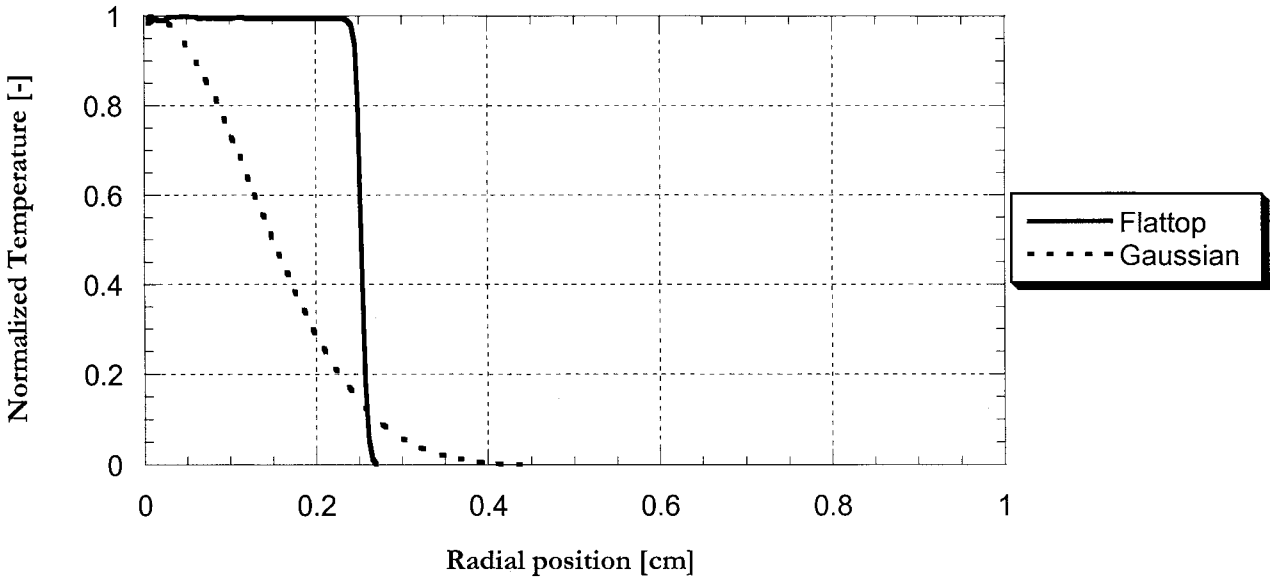

Fig. 6. Normalized temperature profiles at the end of a laser pulse for flattop (solid line) and gaussian (dashed line) beam profiles.

CONCLUSIONS

Theoretical calculations showed that the concept of thermal relaxation time does not adequately provide a measure of time that can be used during multiple-pulse irradiation of tissue. It is necessary to consider the slow temperature decay that occurs for times longer than τ_r. The following equation can be used to estimate τ_{eff}.

$$\tau_{eff} = m\tau_r = \frac{m\delta^2}{4\alpha},$$

where m is the slope of the line fitting τ_{eff} (calculated with Equation (5)) as a function of τ_r. Calculated values of m for six combinations of ΔT_{peak} and ΔT_{base} are provided in Table 3; it is straightforward to calculate m with Equation (5) for other combinations.

REFERENCES

1. Anderson RR, Parrish JA. Selective photothermolysis: precise microsurgery by selective absorption of pulsed radiation. Science 1983;220:524–527.
2. Choi B, Chan EK, Barton JK, Thomsen SL, Welch AJ. Thermographic and histological evaluation of laser skin resurfacing scans. IEEE J Sel Top Quant Elect 1999;5: 1116–1126.
3. Jansen ED, van Leeuwen TG, Motamedi M, Borst C, Welch AJ. Temperature dependence of the absorption coefficient of water for midinfrared laser radiation. Lasers Surg Med 1994; 14:258–268.
4. Walsh JT, Cummings JP. Effect of the dynamic optical properties of water on midinfrared laser ablation. Lasers Surg Med 1994;15:295–305.
5. Choi B, Barton JK, Chan EK, Welch AJ. Imaging of the irradiation of skin with a clinical CO_2 laser system: implications for laser skin resurfacing. Lasers Surg Med 1998;23: 185–193.
6. Jansen ED, Chundru RK, Samanani SA, Tibbetts TA, Welch AJ. Pulsed infrared laser irradiation of biological tissue: effect of pulse duration and repetition rate. Proc SPIE 1993;1882:322–326.
7. Schomacker K, Walsh JT, Flotte T, Deutsch T. Thermal damage produced by high-irradiance continuous wave CO_2 laser cutting of tissue. Lasers Surg Med 1990; 10:74–84.
8. Zweig AD, Meierhofer B, Muller OM, Mischler C, Romano V, Frenz M, Weber HP. Lateral thermal damage along pulsed laser incisions. Lasers Surg Med 1990;10:262–274.
9. Incropera FP, DeWitt DP. Fundamentals of Heat and Mass Transfer. New York: John Wiley; 1996;248–262.
10. Walsh JT, Deutsch TF. Pulsed CO_2 laser tissue ablation: measurement of the ablation rate. Lasers Surg Med 1988; 8:264–275.
11. Brugmans MJP, Kemper J, Gijsbers GHM, van der Meulen FW, van Gemert MJC. Temperature response of biological materials to pulsed non-ablative CO_2 laser irradiation. Lasers Surg Med 1991;11:587–594.
12. Fried NM, Choi B, Welch AJ, Walsh JT Jr. Radiometric surface temperature measurements during dye-assisted laser skin closure: in vitro and in vivo results. Lasers Surg Med 1999; 25:291–303.
13. Walsh JT, Flotte TJ, Anderson RR, Deutsch TF. Pulsed CO_2 laser tissue ablation: effect of tissue type and pulse duration on thermal damage. Lasers Surg Med 1988;8:108–118.
14. Pearce J, Thomsen S. Rate process analysis of thermal damage. In: Welch AJ, van Gemert MJC, editors. Optical-Thermal Response of Laser-Irradiated Tissue. New York: Plenum Press; 1995;561–606.
15. Anvari B, Tanenbaum BS, Milner TE, Kimel S, Svaasand LO, Nelson JS. A theoretical study of the thermal response of skin to cryogen spray cooling and pulsed laser irradiation: implications for treatment of port wine stain birthmarks. Phys Med Biol 1995; 40:1451–1465.
16. Carslaw HS, Jaeger JC. Conduction of Heat in Solids. Oxford: Clarendon Press; 1959;50–91.
17. Duck FA. Physical Properties of Tissue: A Comprehensive Reference Book. London: Academic Press; 1990. P-?
18. Gerstmann M, Linenberg Y, Katzir A, Akselrod S. Char formation in tissue irradiated with a CO_2 laser: model and simulations. Opt Eng 1994;33:2343–2351.
19. Dover JS, Arndt KA. New approaches to the treatment of vascular lesions. Lasers Surg Med 2000;26:158–163.
20. Welch AJ, Wissler EH, Priebe LA. Significance of blood flow in calculations of temperature in laser irradiated tissue. IEEE Trans Biomed Eng 1980;27:164–166.
21. van Gemert MJC, Welch AJ. Time constants in thermal laser medicine. Lasers Surg Med 1989;9:405–421.